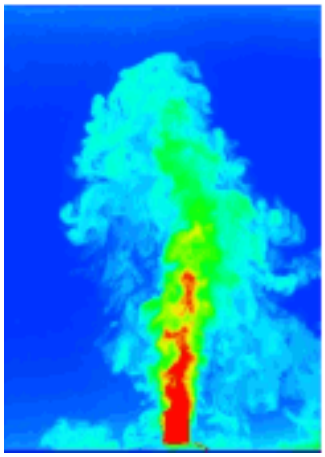

Journal of Turbulence
Publication details, including instructions for authors and subscription information:
http://www.informaworld.com/smpp/title~content=t713665472

Variational assimilation of POD low-order dynamical systems

Juan D'adamo [a]; Nicolas Papadakis [b]; Etienne Mémin [b]; Guillermo Artana [a]
[a] Laboratorio de Fluidodinámica, Universidad de Buenos Aires, Buenos Aires, Argentina
[b] IRISA, Université de Rennes 1, Rennes, France

First Published on: 01 January 2007
To cite this Article: D'adamo, Juan, Papadakis, Nicolas, Mémin, Etienne and Artana, Guillermo (2007) 'Variational assimilation of POD low-order dynamical systems', Journal of Turbulence, Volume 8, Art. No. N9,
To link to this article: DOI: 10.1080/14685240701242385
URL: http://dx.doi.org/10.1080/14685240701242385

Journal of Turbulence
Volume 8, No. 9, 2007

Taylor & Francis
Taylor & Francis Group

Variational assimilation of POD low-order dynamical systems

JUAN D'ADAMO*†, NICOLAS PAPADAKIS‡, ETIENNE MÉMIN‡ and GUILLERMO ARTANA†

†Laboratorio de Fluidodinámica, Universidad de Buenos Aires, Buenos Aires, Argentina
‡IRISA, Université de Rennes 1, Rennes, France

With this work, we propose improvements to the construction of low-order dynamical systems (LODS) for incompressible turbulent external flows. The model is constructed by means of a proper orthogonal decomposition (POD) basis extracted from experimental data. The POD modes are used to formulate an ordinary differential equation (ODE) system or a dynamical system which contains the main features of the flow. This is achieved by applying a Galerkin projection to the Navier–Stokes equations. Usually, the obtained LODS presents stability problems due to modes truncation and numerical uncertainties, specially when working on experimental data. We perform the model closure with a variational method, data assimilation, which refines the state variables within an iterative scheme. The technique allows as to correct the dynamic system coefficients and to identify and ameliorate the issued experimental data.

Keywords: Low-order dynamical systems; Proper orthogonal decomposition; Variational assimilation; Dynamic system coefficients; Incompressible cylinder flow; PIV filtering

1. Introduction

The reduction of the Navier–Stokes equation to a system of ordinary differential equation (ODE) has been largely studied by the computational fluid dynamics (CFD) community. With different tools developed in this domain, it has been possible to reproduce or predict diverse flow characteristics with a large detail. However, the computational cost of these calculations becomes higher as the Reynolds number increases and when turbulent models are considered.

For these reasons, for a couple of years, different research efforts have been tried to deal with the same problem through the so-called low-dimensional dynamic models (LODS) or reduced order models. The goal, which is here less ambitious than a complete flow numerical simulation, consists in capturing and representing the essential characteristics of the flow. These methods aim at describing only coherent structures dynamics, sacrificing all the flows detailed structures.

Some scenarios where these models are of major interest are in flow control applications where simple systems are required. Actuation on coherent structures may be largely amplified producing important modifications of the flow characteristics as it can take place in processes such as boundary layer separation, vortex shedding, transition to turbulence, etc. Another field of application of LODS concerns computational optimization problems where one seeks to avoid the repetition of complete CFD calculations for different initial conditions or for slightly different Reynolds numbers. Working with adequate LODS would accelerate the tasks in these

*Corresponding author. E-mail: jdadamo@fi.uba.ar

Journal of Turbulence
ISSN: 1468-5248 (online only)
http://www.tandf.co.uk/journals
DOI: 10.1080/14685240701242385

cases. Furthermore, LODS can be helpful in experimental fluid mechanics as they allow as to organize and interpret large data realizations, and to extract a model from them.

A way to obtain LODS is by means of the proper orthogonal decomposition (POD) technique. Also known as Karhunen–Loève decomposition, singular value decomposition, principal components analysis, POD was first introduced in the context of turbulence by Lumley [14]. It has been used by different authors (see for instance a review [11]) as a method to obtain approximate descriptions of the large scale or coherent structures in laminar and turbulent flows. Without any a priori hypotheses on the flow, the POD method provides a flow representation in terms of a mean and a linear combination of basis functions, or modes, ordered decreasingly by their kinetic energy content.

The estimation of the POD basis vectors relies on a set of flow-field realizations $u(X, t)$ which can either be obtained from CFD or experiments. Such a technique has been proposed for many situations arising in a fluid dynamic problem: a non-exhaustive list includes analyses of shear layers [18], transition in boundary layers [19], turbulent boundary layers [1], flow in a channel [8], flow around a circular cylinder [8], cavity flows [5], etc.

Experiment-based POD models have to cope with numerical instability. Such a problem is usually tackled by adding forced artificial closure terms [3, 4]. These instabilities come mainly from evaluation of inner products and derivatives on the sparse grid of experimental realization. Efforts to overcome this kind of problems were made by different approaches. Particularly a polynomial identification technique was proposed firstly in [3], and than in [16, 17]. The dynamic system coefficients are estimated not directly by Galerkin projection but from least-squares fitting of experimental data. The idea has also been proposed in [6] where the authors study the optimal control method. However, this approach considers that the dynamical model is perfect and the solution is only monitored with the initial condition.

In this work, we propose to improve such solution, by relying on the variational data assimilation framework. Such a framework enables us to estimate the state of variables of interest characterizing the flow under observation (such as pressure, density, velocity components, salinity, etc.) given a dynamical law and sparse and possibly noisy measurements at different time instants. This approach also allows us to handle very large scale systems and as such are intensively used in environmental sciences [2, 13, 21–23] for atmospheric or oceanic analysis and forecasting. We rely on this technique to estimate in batch mode the complete trajectories along an image sequence of POD modes. As we will show it, such a method allows us to refine a first crude initial estimate obtained through polynomial identification. The method couples an imperfect noisy dynamic model with the whole sequence of observations. Given the whole trajectories of POD modes, the dynamic system coefficients initially provided by noisy PIV data can then be re-estimated from a mean square fitting of the assimilation results. As demonstrated in the experimental section, the technique we propose enables the reconstruction of the most salient characteristics of the flows for a long time range. The stability and the accuracy of the LODS are significantly improved.

The remainder of the paper is organized as follows. First, the necessary basis to the construction of a flow POD representation from particle image velocimetry (PIV) observations is recalled in section 2.1. The way PIV observations can be filtered and improved is described in section 2.2. The obtention of LODS from POD basis is described in section 2.3. In section 2.4, we describe the experimental setup we used in this work, and discuss first results obtained through the polynomial identification technique. Variational data assimilation principles are presented in section 3. The technique we propose for LODS identification is presented in section 3.2. Finally, results obtained for the POD-assimilation scheme are given and studied in section 5.

2. Proper orthogonal decomposition

2.1 *POD basis*

The POD method has been widely used by different authors as a technique to obtain approximate descriptions of the large scale or coherent structures in laminar and turbulent flows. Given an ensemble $u(x, t_i)$ obtained experimentally, belonging to M different discrete instants, POD provides M mutually orthogonal basic functions, or *modes*, $\phi_i(x)$, which are optimal with respect to average kinetic energy representation of the flux.

Considering such a decomposition enables us to write the velocity field as an average $\bar{u}$ with fluctuations captured by a finite set of modes:

$$u(x, t) = \bar{u} + \sum_{i=1}^{M} a_i(t)\phi_i(x). \tag{1}$$

Being fields of finite kinetic energy, $u \in L^2$ and denoting by $(,)$ the inner product of functions defined in $L^2(S)$:

$$(u, \psi) = \int_S u\psi ds, \tag{2}$$

where S represents the spatial domain occupied by the flux. Seeking a subspace such that the projection of $u(x, t_i)$ on it is optimal along the sampling time comes to find an ensemble of functions that maximize

$$\frac{\langle |(u, \psi)|^2 \rangle}{(\psi, \psi)},$$

where $\langle \bullet \rangle$ denotes a temporal average. It can be demonstrated [11] that the optimal functions ϕ also satisfy the following eigenvalue problem:

$$\int_S K(x, x')\phi_k(x)dx = \phi_k(x)\lambda_k, \tag{3}$$

with

$$K(x, x') = \langle u(x, t)u(x', t) \rangle = \frac{1}{M} \sum_{i=1}^{M} u(x, t_i)u(x', t_i).$$

To solve our problem, it is easier numerically to follow Sirovich's snapshots method [20], which states that each spatial mode ϕ can be constructed by a superposition of the velocities fields:

$$\phi_k(x) = \sum_{i=1}^{M} u(x, t_i)a_k(t_i).$$

Projecting (3) into a snapshot $u(x, t_j)$, we obtain another eigenvalue problem, whose eigenvectors are the temporal modes a_k.

2.2 *Gappy POD*

A problem arises when the snapshot $u(x, t_i)$ given through a PIV technique contains erroneous vectors. To correct this deficiency, Everson and Sirovich [9] have proposed an iterative scheme. We consider the same kind of setup in this work. It first consists in creating an ensemble of

masks $m(x, t_i)$, with values either zero or unity if there is a wrong or a reliable vector $u(x, t_i)$ at position x of time t_i. We can respectively write the velocity fields with data missing, $\tilde{u}(x, t_i)$, in terms of the masks $m(x, t_i)$ and the complete velocity fields $u(x, t_i)$:

$$\tilde{u}(x, t_i) = m(x, t_i)u(x, t_i).$$

To compute the temporal average of $\tilde{u}(x, t_i)$, we only take into account the reliable values,

$$\tilde{u}_m(x) = \langle \tilde{u}(x, t_i) \rangle = \frac{1}{\sum m(x, t_i)} \sum_i m(x, t_i)u(x, t_i).$$

A first correction of the erroneous data is achieved by replacing erroneous values by the temporal average. The reliable data, whose $(x, t_i) \in S$, remain without changes. So for each $(x, t_i) \notin S$

$$\tilde{u}^{(0)}(x, t_i) = \tilde{u}_m(x).$$

With these corrected values, a POD can be settled to provide an initial set of spatial and temporal modes: $\phi^{(0)}(x) = \{\phi_k^{(0)}(x), k = 1, \ldots, M\}$ and $a^{(0)}(t_i) = \{a_k^{(0)}(t_i), k = 1, \ldots, M\}$.

The restored vector field at the following iteration, $\tilde{u}^{(1)}(x, t_i)$, is obtained by fitting each member of the original ensemble, $\tilde{u}(x, t_i)$, to a superposition of M eigenfunctions $\phi_k^{(0)}(x)$ as follows:

$$\tilde{u}(x, t_i) = \sum_{k=1}^{M} a_k^{(1)}(t_i)\phi_k^{(0)}(x) \qquad \forall (x, t_i) \in S,$$

$$\left(\phi_j^{(0)}, \tilde{u}(x, t_i)\right) = \left(\phi_j^{(0)}, \sum_{k=1}^{M} a_k^{(1)}(t_i)\phi_k^{(0)}(x)\right).$$

From ϕ_k orthonormality, we can write

$$a_j^{(1)}(t_i) = \left(\phi_j^{(0)}, \tilde{u}(x, t_i)\right) \qquad \forall j = 1, \ldots, M. \tag{4}$$

From the set of estimated temporal modes $a^{(1)}(t_i)$ and the basis functions $\phi^{(0)}(x)$, the updated set of velocity values $\tilde{u}^{(1)}$ is obtained. This process is iteratively repeated until a convergence criterion is met. Further details on this method can be found in [24] and in [7] for the particuliar case of PIV data.

2.3 *Formulation of a low-order dynamical system (LODS): Galerkin projection*

From the modal decomposition, it is possible to consider a truncated model with s modes to approximate the velocity field $u(x, t_i)$, with $x \in S, 1 \leq i \leq M$ and $s \ll M$. From the properties of POD, it is easy to measure the kinetic energy percentage contained in this model:

$$\frac{\sum_{i=1}^{s} \lambda_i}{\sum_{i=1}^{M} \lambda_i}.$$

A Galerkin projection enables us to rewrite a partial differential equation (PDE) system as a system of ordinary differential equations (ODE). According to this procedure, the functions which define the original equation are projected on a finite-dimensional subspace of the phase space (in this case, the subspace generated by the first s modes). Following a scheme proposed by Rajaee *et al.* [18], we project the Navier–Stokes equations under

the Reynolds decomposition, in order to have an explicit expression for the fluctuating quantities:

$$\left(\frac{\partial u'}{\partial t} + u'\nabla\bar{u} + \bar{u}\nabla u' + u'\nabla u' - \overline{u'\nabla u'} + \frac{\nabla p'}{\rho} - \nu\nabla^2(\bar{u} + u'),\ \phi_j\right) = 0. \tag{5}$$

These equations are obtained by separating the flow velocity into mean $\bar{u}$ and fluctuating u' parts: $u = \bar{u} + u'$. Rewriting (5) in terms of POD (1), the resulting equation is a quadratic ODE of order 1. For every $j \leq s$ mode, the system reads

$$\frac{da_k}{dt} = F(a_k) = i_k + \sum_{i=1}^{s} l_{ik}a_i + \sum_{i=1}^{s}\sum_{j=i}^{s} a_i c_{ijk} a_j \qquad k = 1, \ldots, s \tag{6}$$

where

$$l_{ij} = \int_S \bar{u}\nabla\phi_i\phi_j ds + \int_S \phi_i\nabla\bar{u}\phi_j ds - \int_S \frac{1}{Re}\Delta\phi_i\phi_j ds, \tag{7}$$

$$c_{ijk} = \int_S \phi_j\nabla\phi_i\phi_k ds, \tag{8}$$

$$i_k = \int_S \nabla p'\phi_k ds - \frac{1}{Re}\int_S \Delta\bar{u}\phi_k ds - \sum_{j=1}^{s}\lambda_j \int_S \phi_j\nabla\phi_j\phi_k ds. \tag{9}$$

Regarding these expresions, (7) describes the interaction between the mean flow and fluctuating field; it also includes viscous effects associated with the fluctuating velocity field. Nonlinear effects are reported by (8). The independent term (9) takes into account the pressure field influence, mean flow dissipation, and the convective term of the modes.

Boundary conditions and symmetry make the pressure term vanish in a particular case of wake flow. As a matter of fact, each of the mode functions satisfies the continuity equation, to give

$$\int_S \nabla p'\phi_k ds = \oint_C p'\phi_k dc,$$

where C is the boundary curve of domain S. Works of Deane [8] and Noack [15] demonstrated that for wake flow configuration, the latter expression is negligible compared to the other terms. Nevertheless, the inclusion of the p' term can be modelled through an additional quadratic expression of the temporal modes a, which is achieved by polynomial identification. A noisy version of the momentum equation (6) can also be considered to deal with the p' term. Such a situation will be the core of the POD-assimilation technique. Direct calculation of each term of the system (6) can be avoided by using polynomial identification, described as follows.

2.4 *First results and LODS adjustment*

A common problem regarding reduced order models is how to model the unresolved modes of the flow. Although we have a model that enables us to represent the most energetic structures, associated with the flow greatest scales, the smaller ones should also be included as they play an important role in the dissipation process. Practical implementations showed that (6) can only be solved for a short time range when neglecting the effect of small scales.

This problem was first pointed out by Holmes *et al*. [11], where a polynomial similar to (6) is modified after an estimation of the incoherent, unresolved modes in terms of the resolved modes. Long time behaviour of LODS solution can be seen as an attracting set. We can consider every observation a_i as an element of this set. Another way to refine the model, first

proposed by Braud [3, 4], consists in estimating the polynomial coefficients through least-squares fitting. Provided each observation a_i and its derivative $\dot{a}_i$, we can write (6) as the solution of a linear system. This polynomial identification technique has been tested on the Lorenz dynamical model and on POD dynamical systems. This method presents the great advantage to avoid the accurate computation of the basis functions' spatial derivatives that are required to construct the projected model (7)–(9). It can be pointed out also that even if closed pairs of observation $a_i(t_k)$ and $a_i(t_{k+1})$ are needed to compute the temporal derivative (6), those pairs are not required to be correlated [11].

The experimental configuration we settled for this work consists of a flow around a circular cylinder at low Reynolds number, $\mathrm{Re} = 125$. The velocity measurements have been done in a closed loop wind tunnel with a probe section of 18×18 cm^2. A 2 cm diameter cylinder was placed in order to have snapshots of 5 by 4 diameters. We chose it regarding the wake structures we wanted to identify.

As for the PIV system, we used a Pixelfly PCO VGA camera, with a resolution of 640×240 pixels, 1/100 s of time between images. A green laser Intelite GM32-150IH, 150 mW, combined with a rotating polyhedric mirror, was used to provide illumination on the probe section.

The algorithms used in this work belong to GPIV software [10] which is under GNU General Public License. We have considered for our images a two-step grid refinement, so the final interrogation size is 16×16 pixels with a 50% overlapping.

The time resolution was suitable to recover the flow dynamics, in a way that the vortex shedding frequencies are lower than the acquisition frequency. Although the technique does not require time correlated data, this condition allowed us to validate our models. A set of 1000 images was used to construct the reduced order model. Convergence on the mean and modes calculation was verified. Indeed, the difference between the resulting mean and modes for a set of 750 snapshots and for a set of 1000 snapshots was estimated by projections as defined in (2). This allowed us to evaluate $1 - (\phi_i^{750}, \phi_i^{1000})$. The maximum difference was of the order of 0.5% for all the modes considered.

The data have been filtered by the gappy technique and then the fluctuating velocity field was decomposed with POD. As expected in a low turbulence flow, the first modes concentrate the most of the fluctuating kinetic energy as is shown in figure 1. As illustrated in figure 2, the

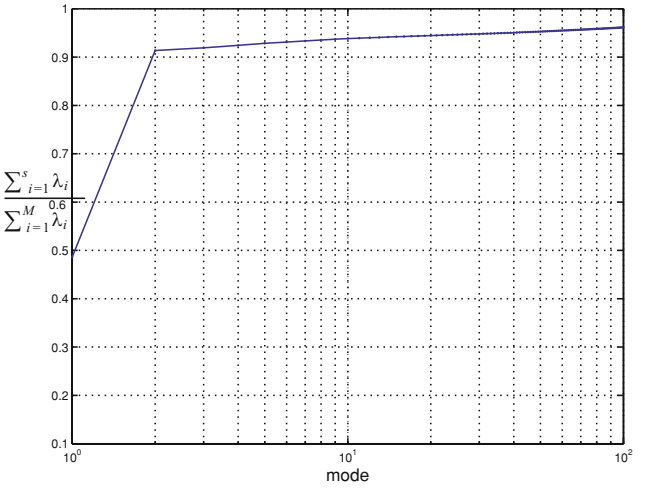

Figure 1. Partial amount of kinetic energy contained in s modes.

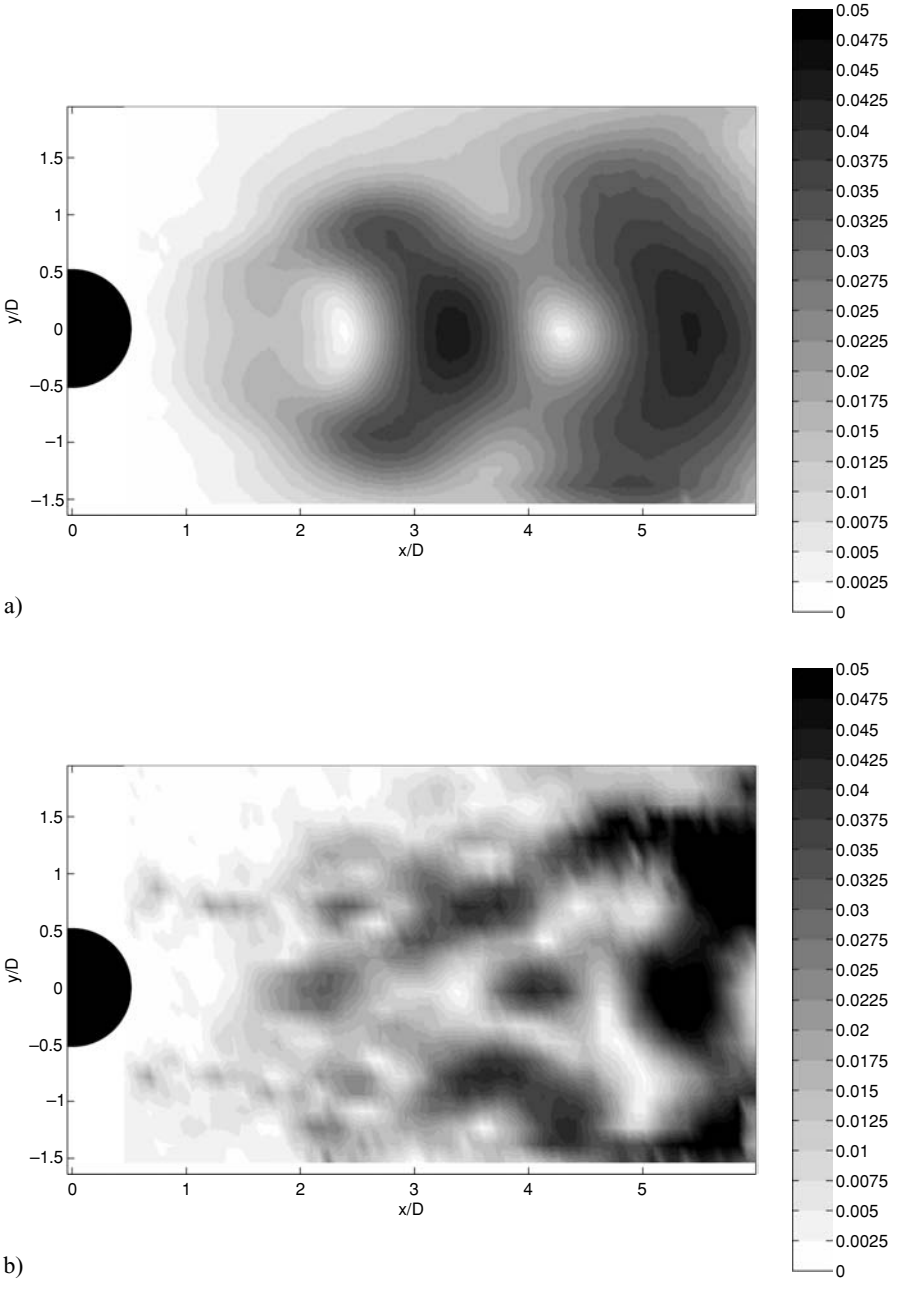

Figure 2. Contour maps of spatial modes: (a)$\phi_1(x)$; (b)$\phi_3(x)$.

spatial modes extracted from the decomposition represent the recurrent structures of the flow. We can observe that structures with higher fluctuating kinetic energy concentration results appear to be more spatially organized.

In a first experiment, we choose to keep only $s = 2$ modes to be sured to recover the 91% of kinetic energy. The coefficients of equation (6) have been estimated by polynomial identification based on mean squares fitting. The corresponding solution of the LODS is plotted

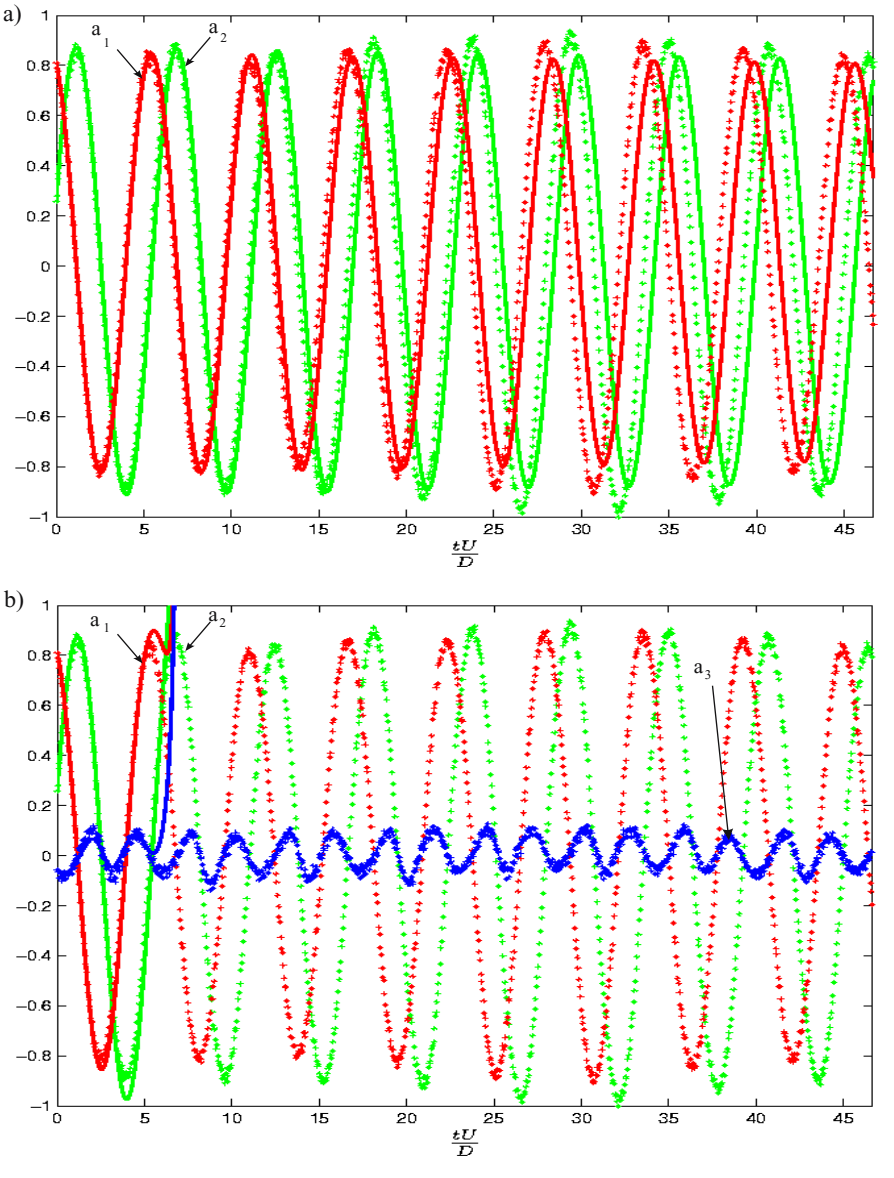

Figure 3. First estimation of the ODE. Comparison between ODE solution (solid line) and original data (symbols). (a) For $s = 2$; (b) solution diverges for systems $s \geq 4$.

in figure 3(a) where we have plotted also the original data for comparison purpose. Although the short term behaviour of the model is quite accurate, significant errors in magnitude and phase appear very quicly. These errors amplify as time goes by. For a system with a larger number of modes the solution does not converge at all. This is illustrated in figure 3(b) where we have plotted the solution for a LODS with four modes.

In order to improve the estimation of the temporal modes we will place ourselves within the framework of variational data assimilation. We briefly describe its principles in the next section.

3. Data assimilation principle

3.1 *Assimilation for well-posed dynamical models*

Data assimilation is a technique that enables us to perform the estimation over time of state variables representing a system of interest. The method enables us to perform a smoothing of noisy measurements of the system's state according to a given initial state of the system and a dynamic law. Let us note that $X \in \Xi$ in the state variable of interest. This variable may represent any quantities associated with the observed flow such as temperature, velocity, vorticity, pressure, etc. Assuming that the evolution in time of these quantities is described through a (nonlinear) differential model $\mathbb{M}$ we get the following dynamical system:

$$\begin{cases} \dfrac{dX}{dt} + \mathbb{M}(X, s) = 0 \\ X(t_0) = X_0. \end{cases} \tag{10}$$

This system is monitored by a control variable $r = (s, X_0) \in P$, defined in control space. This control variable may be set to the initial condition or to any free parameter of the evolution law. Let us also assume that some observations $Y \in O_{\text{obs}}$ of the state variable components are available. These observations may live in a different space (a reduced space for instance) from the state variable. We will nevertheless assume that there exists a matrix operator H that goes from the variable space to the observation space. A least-squares estimation of the control variable regarding the whole sequence of measurements available within a considered time range comes to minimize with respect to the control variable a cost function of the following form:

$$J(r) = \frac{1}{2} \int_{t_0}^{t_f} ||Y - HX(s, X_0)||^2 dt. \tag{11}$$

3.1.1 Minimization of the functional. A first approach consists in computing the functional gradient through finite differences:

$$\nabla_r \simeq \frac{J(r + \epsilon e_k) - J(r)}{\epsilon},$$

where $\epsilon \in \mathbb{R}$ is an infinitesimal perturbation and $\{e_k, k = 1, \ldots, p\}$ denotes the unitary basis vectors of the control space. Such a computation is impractical for space of large dimensions since it requires p integrations of the evolution model for each required value of the gradient functional. *Adjoint models* as introduced first in meteorology by Le Dimet and Talagrand in [13] will allow us to compute the gradient functional in a single integration. Denoting $\delta r = X(dr)$ a perturbation of the solution correponding to $dr \in P$ we have

$$\begin{aligned} \delta J &= \langle \nabla J_r, \delta r \rangle \\ &= -\langle H^T (Y - H(X(s, X_0))), \delta r \rangle \end{aligned} \tag{12}$$

This perturbation evolves according to

$$\frac{d}{dt}\delta r + \partial_r \mathbb{M} \delta r = \frac{d}{dt}\delta r + \partial_{X_o} \mathbb{M} \delta X_0 + \partial_s \mathbb{M} \delta s = 0.$$

The right part of this linear evolution law involves the so-called *tangent linear model* of $\mathbb{M}$. It is defined as the Gâteaux derivative at point X of the operator $\mathbb{M}$:

$$\lim_{\beta \to 0} \frac{d\mathbb{M}(X + \beta\theta)}{d\beta} = \partial_X \mathbb{M}\theta. \tag{13}$$

This linear operator describes how arbitrary perturbations of the control evolve in time. Now considering the inner product of the tangent linear model with an arbitrary vector $\boldsymbol{\lambda}$ and an integration by part leads to

$$\int_O^T \left\langle \frac{d}{dt}\delta r, \lambda \right\rangle dt = \langle \delta r(T), \lambda(T) \rangle - \langle \delta r(0), \lambda(0) \rangle - \int_O^T \left\langle \delta r, \frac{d}{dt}\lambda \right\rangle dt,$$

Imposing that $\lambda(T) = 0$, introducing of the tangent linear model and using the definition of an adjoint operator associated with a given inner product (i.e. $\langle x, \mathcal{L}y \rangle = \langle \mathcal{L}^* x, y \rangle$), we get:

$$\begin{aligned} \langle \delta r(0), \boldsymbol{\lambda}(0) \rangle &= \int_O^T \langle \delta r, \partial_r \mathbb{M}^* \lambda \rangle dt - \int_O^T \left\langle \delta u, \frac{d\lambda}{dt} \right\rangle \\ &= \int_O^T \left\langle \delta r, -\frac{d\lambda}{dt} + \partial_r \mathbb{M}^* \lambda \right\rangle dt. \end{aligned}$$

We define the adjoint model requiring in addition that

$$-\frac{d\lambda}{dt} + \partial_r \mathbb{M}^* \lambda = H^T (Y - H(X(s, X_0))).$$

This adjoint model together with the definition of the gradient functional (12) enables us to write

$$\nabla_r J = -\lambda(0).$$

As a consequence, the functional gradient can be computed as a single backward integration of an adjoint model. The value of this adjoint variable at the initial time provides the value of the gradient. This first approach is widely used in environmental sciences for the analysis of geophysical flows. However, these methods rely on a perfect dynamical model.

3.2 *Assimilation for noisy dynamical models*

Considering imperfect models, defined up to a Gaussian noise, we have to consider an optimization problem where the control variable is constituted by the whole trajectory of the state variable. This is the kind of problem we are facing in this work.

The ingredients of the new data assimilation problem are now composed by an imperfect dynamic model of the target, an initialization of the state variable and an observation equation which relates the state variables to some measurements:

$$\begin{cases} \dfrac{dX}{dt} + \mathbb{M}(X) = \nu(t) \\ X(t_0) = X_0 + \eta \\ Y(t) = HX + \epsilon(t). \end{cases} \tag{14}$$

In these three equations η, ν and ϵ are time varying zero mean Gaussian noise vector functions. They are respectively associated with covariance matrices $W(t, t')$, B and $R(t, t')$. The noise functions represent the different errors involved in the different components of the system (i.e.

model errors, initialization errors and measurement errors) and are assumed to be uncorrelated in time. The goal is to minimize the new functional, which considers the noise of the model:

$$J(X) = \frac{1}{2}\int_{t_0}^{t_f} \left|\left|\frac{dX}{dt} + \mathbb{M}(X)\right|\right|_W^2 dt + \frac{1}{2}||X(t_0) - X_0||_B^2 + \frac{1}{2}\int_{t_0}^{t_f} ||HX(U,V) - Y||_R^2 dt. \tag{15}$$

The minimization has now to be done according to the state variable X.

3.2.1 Minimization of the functional of the noisy model. A minimizer X of functional J is also a minimum of a cost function $J(X+\beta\theta(t))$, where $\theta(t)$ belongs to a space of admissible function and β is a positive parameter. In other words, X must cancel the directional derivative:

$$\delta J_X(\theta) = \lim_{\beta\to 0} \frac{dJ(X+\beta\theta(t))}{d\beta} = 0.$$

The functional with an infinitesimal perturbation read:

$$\begin{aligned} J(X+\beta\theta) = {} & \frac{1}{2}\int_{t_0}^{t_f} \left(\frac{dX}{dt} + \beta\frac{d\theta}{dt} + \mathbb{M}(X+\beta\theta)\right)^T \int_{t_0}^{t_f} W^{-1}(t,t') \\ & \times \left(\frac{dX}{dt} + \beta\frac{d\theta}{dt} + \mathbb{M}(X+\beta\theta)\right)dt'dt + \frac{1}{2}(X+\beta\theta-X_0)^T B^{-1}(X+\beta\theta-X_0) \\ & + \frac{1}{2}\int_{t_0}^{t_f}\int_{t_0}^{t_f} (Y - H(X+\beta\theta))^T(t) R^{-1}(t,t')(Y - H(X+\beta\theta))(t')dt'dt. \end{aligned} \tag{16}$$

In order to derive a practical definition of the gradient functional we introduce again an adjoint variable $\boldsymbol{\lambda}$ defined as

$$\boldsymbol{\lambda}(t) = \int_{t_0}^{t_f} W^{-1}(t,t')\left(\frac{dX}{dt} + \mathbb{M}(X)\right)dt'. \tag{17}$$

By taking the limit $\beta \to 0$, the derivative of expression (16) then reads

$$\begin{aligned} \lim_{\beta\to 0}\frac{dJ}{d\beta} = {} & \int_{t_0}^{t_f} \left(\frac{d\theta}{dt} + \partial_X\mathbb{M}\theta\right)^T(t)\boldsymbol{\lambda}(t)dt + \theta^T(t_0)B^{-1}(X(t_0) - X_0) \\ & - \int_{t_0}^{t_f}\int_{t_0}^{t_f} H^T\theta^T(t)R^{-1}(t,t')(Y - HX)(t')dt'dt = 0. \end{aligned} \tag{18}$$

Applying integrations by parts, we can get rid of the partial derivatives of the admissible function θ in expression (18). This equation (18) can then be rewritten as

$$\begin{aligned} \lim_{\beta\to 0}\frac{dJ}{d\beta} = {} & \theta^T(t_f)\boldsymbol{\lambda}(t_f) + \theta^T(t_0)[B^{-1}(X(t_0) - X_0) - \boldsymbol{\lambda}(t_0)] \\ & + \int_{t_0}^{t_f} \theta^T(t)\left[\left(-\frac{d\boldsymbol{\lambda}}{dt} + \partial_X\mathbb{M}^*\boldsymbol{\lambda}\right)(t) - \int_{t_0}^{t_f} H^T R^{-1}(t,t')(Y - HX)(t')dt'\right]dt = 0. \end{aligned} \tag{19}$$

Since the functional derivative must be null for arbitrary independent admissible functions in the three integrals of expression (19), all the other members appearing in the three integral terms must be identically null.

3.2.2 PDE system for the functional minimization. The PDE system associated with the functional minimization obtained from (19) is a coupled system of forward and backward

PDEs with two initial and end conditions:

$$\lambda(t_f) = 0 \tag{20}$$

$$-\frac{d\lambda}{dt} + \partial_X \mathbb{M}^* \lambda = \int_{t_0}^{t_f} \partial_X \mathbb{H}^* R^{-1}(t, t')(Y - \mathbb{H}(X))dt' \tag{21}$$

$$\lambda(t_0) = B^{-1}(X(t_0) - X_0) \tag{22}$$

$$\frac{dX}{dt} + \mathbb{M}(X) = \int_{t_0}^{t_f} W(t, t')\lambda(t')dt'. \tag{23}$$

The forward equation (23) corresponds to the definition of the adjoint variable (17) and has been obtained introducing W, the pseudo-inverse of W^{-1}, defined as [2]

$$\int_{t_0}^{t_f} W(t, t')W^{-1}(t', t'')dt' = \delta(t - t'').$$

We can see that equation (20) constitutes an explicit end condition for the adjoint evolution model equation (21). As mentioned previously, the adjoint evolution model has to be integrated backward from the end condition assuming the knowledge of an initial guess for X to compute the discrepancy $Y - \mathbb{H}(X)$. This model is defined from the expression of the *adjoint evolution operator*. A discrete expression of this operator can be easily obtained when the discretization of the linear tangent operator can be expressed as a matrix. It consists in that case of the transpose of that matrix. Knowing a first solution of the adjoint variable, an initial condition for the state variable can be obtained from (22) and a pseudo-inverse expression of the covariance matrix B. From this initial condition, (23) can be finally integrated forward.

The previous system can be slightly modified to produce an adequate initial guess for the state variable. Considering a function of state increments linking the state function and an initial condition function, $\delta X = X - X_0$, and linearizing the operator $\mathbb{M}$ around the initial condition function X_0[†]:

$$\mathbb{M}(X) = \mathbb{M}(X_0) + \partial_{X_0}\mathbb{M}(\delta X),$$

we can split equation (23) into two PDEs with an explicit initial condition:

$$X(t_0) = X_0 \tag{24}$$

$$\frac{dX_0}{dt} + \mathbb{M}(X_0) = 0 \tag{25}$$

$$\frac{d\delta X}{dt} + \partial_{X_0}\mathbb{M}\delta X = \int_{t_0}^{t_f} W(t, t')\lambda(t')dt'. \tag{26}$$

Let us note that if the model is assumed to be perfect as in the introduction case, we would have $W = 0$ and recover the inital system of equation. The incremental system with associated with an imperfect dynamical model highlights a major difference with the classic assimilation scheme. As W is not null, the solution is updated with all the values of the adjoint variable trajectory.

Combining equations (20)–(22) and (24)–(26) leads to the final assimilation algorithm. The method consists first in a forward integration of the initial condition X_0 with the state variable's evolution model (25). The current solution is then corrected by performing a backward integration (20), (21) of the adjoint variable. The evolution of $\boldsymbol{\lambda}$ is guided by a discrepancy

[†]The linearization is equivalent to the Gâteaux derivative defined previously.

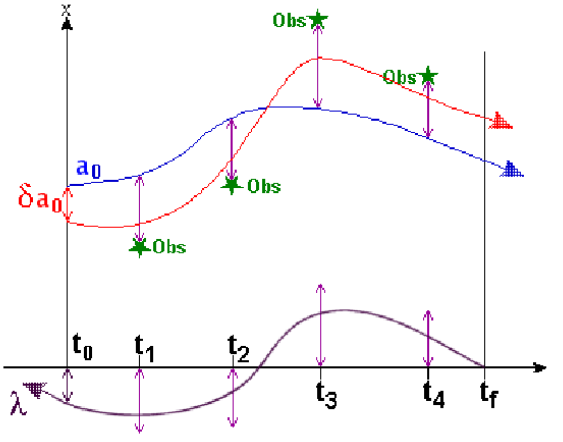

Figure 4. Assimilation algorithm principle.

measure between the observation and the estimate: $Y - HX$. The initial condition is then updated through equation (22) and a forward integration of the increment δX is realized through equation (26). The estimation is updated at each step: $X := X + \delta X$. The overall process is iteratively repeated until convergence (see figure 4).

4. Application to the LODS

We describe now how such a framework has been applied to the problem of LODS coefficient estimation.

4.1 *Description of the problem*

We want to use the assimilation system in order to enhance the estimation of the coefficient of the LODS. The following LODS-assimilation problem is introduced:

$$\begin{cases} \dfrac{da}{dt} + \mathbb{M}(a) = \nu(t) \\ a(t_0) = a_0 + \eta \\ Y(t) = \mathbb{H}(a) + \epsilon(t). \end{cases} \tag{27}$$

The right-hand side of the first equation describes, through a differential operator $\mathbb{M}$, the evolution of the state function $a = [a_1(t) \cdots a_s(t)]$ composed of the POD temporal coefficients and defined over the whole time range $[t_0; t_f]$. In our case, the model and the associated operator $\mathbb{M}$ are given through equation (6):

$$\frac{da_k(t)}{dt} = \underbrace{i_k + \sum_{i=1}^{s} l_{ik} a_i + \sum_{i=1}^{s}\sum_{j=1}^{s} a_i c_{ijk} a_j}_{-\mathbb{M}(a_k)} \qquad k = 1, \ldots, s. \tag{28}$$

We assume here that considering an evolution model defined up to a Gaussian variable will allow us to model the effect of unresolved modes of the flow and therefore will enable a better accuracy of the recovered solution on a longer time range. The second equation of the system

fixes an initial condition for the state vector through a given initialization a_0. The last equation links an observation function $Y(t)$, constituted by noisy measurements of the state function components, to the state function. In the current application, the measurements are given by the temporal modes estimated from PIV snapshots and a POD technique. As the measurements belong to same space as the state variable we have $H = Id$ in this case.

4.2 *Linear tangent operator*

In this section, we describe the discretization of the linear tangent operator of the considered reduced dynamical system. Starting from the dynamical equation

$$\frac{da_k(t)}{dt} = i_k + \sum_{i=1}^{s} l_{ik}a_i + \sum_{i=1}^{s}\sum_{j=1}^{s} a_i c_{ijk} a_j = -\mathbb{M}(a_k) \quad k = 1, \ldots, s, \tag{29}$$

we simply have to compute the linear tangent operator $\partial_a \mathbb{M}(\theta)$ for a small perturbation $\theta(t) = [\theta_1(t) \cdots \theta_s(t)]^T$:

$$\partial_a \mathbb{M}(\theta_k) = -\left[\sum_{i=1}^{s} l_{ik}\theta_i + \sum_{i=1}^{s}\sum_{j=1}^{s}(a_i c_{ijk}\theta_j + \theta_i c_{ijk} a_j)\right] \quad k = 1, \ldots, s. \tag{30}$$

And finally

$$\partial_a \mathbb{M}(\theta_k) = -\left[\sum_{i=1}^{s} l_{ik}\theta_i + 2\sum_{i=1}^{s}\sum_{j=1}^{s} a_i c_{ijk}\theta_j\right] \quad k = 1, \ldots, s. \tag{31}$$

Hence, we obtain

$$\partial_a \mathbb{M}(\theta) = -(L + 2C)\theta. \tag{32}$$

where L and C are matrices $(s \times s)$:

$$L = \begin{bmatrix} l_{11} & l_{12} & \cdots & l_{1s} \\ l_{21} & l_{22} & \cdots & l_{2s} \\ \vdots & \vdots & \cdots & \vdots \\ l_{s1} & l_{s2} & \cdots & l_{ss} \end{bmatrix}, \tag{33}$$

$$C = \begin{bmatrix} \sum_{j=1}^{s} a_j c_{1j1} & \sum_{j=1}^{s} a_j c_{2j1} & \cdots & \sum_{j=1}^{s} a_j c_{sj1} \\ \sum_{j=1}^{s} a_j c_{1j2} & \sum_{j=1}^{s} a_j c_{2j2} & \cdots & \sum_{j=1}^{s} a_j c_{sj2} \\ \vdots & \vdots & \cdots & \vdots \\ \sum_{j=1}^{s} a_j c_{1js} & \sum_{j=1}^{s} a_j c_{2js} & \cdots & \sum_{j=1}^{s} a_j c_{sjs} \end{bmatrix}. \tag{34}$$

4.3 *Convergence and numerical stability*

Recalling that Euler–Lagrange equations consist of the functional J around a small perturbation θ:

$$J(a+\theta) = J(a) + \nabla J \cdot \theta, \tag{35}$$

and that equation (19) gives us an analytic representation of the second part of (35):

$$\nabla J = \lim_{\alpha \to 0} \frac{dJ}{d\alpha},$$

allows us to define a natural convergence criterion:

$$\nabla J \cdot \theta < \epsilon. \tag{36}$$

These two expressions of the gradient provide a practical way to determine if the adjoint equation is well discretized:

$$\lim_{\alpha \to 0} \frac{J(a+\alpha\theta) - J(a)}{\alpha \nabla J \cdot \theta} \to 1. \tag{37}$$

The adjoint computation of the functional gradient is here compared to implemention of finite differences. We have checked the validity of our implementation considering this test on a set of real data. The curve showing the ratio for different values of α is presented in figure 5. It can be observed that our discretization is valid up to a 10^{-8} variation. This bound is due to the numerical round-off errors. This study gives us an ad hoc way to set the convergence threshold in equation (36). For the present study, we fixed it to $\epsilon = 10^{-7}$.

5. Results

In this section, we present and analyse results obtained for the assimilation of POD modes.

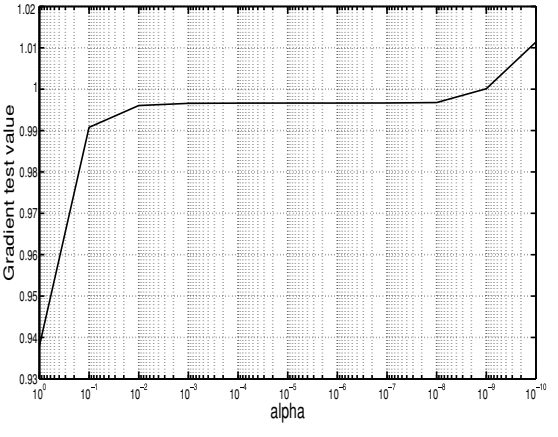

Figure 5. Gradient test realized with $\alpha \to 0$.

5.1 *Analysis of robustness*

As mentioned in the previous section, it is crucial for the assimilation technique associated with imperfect evolution models to have good initial state trajectory. This first guess can be provided by proposing a good initialization of the state vector at the initial state and integrating this initial condition with the model dynamics. Such initial trajectories of the state variable can also be provided by other estimation techniques. In these works, the initial trajectory is assumed to be provided through the polynomial identification technique described in section 2.4. In the

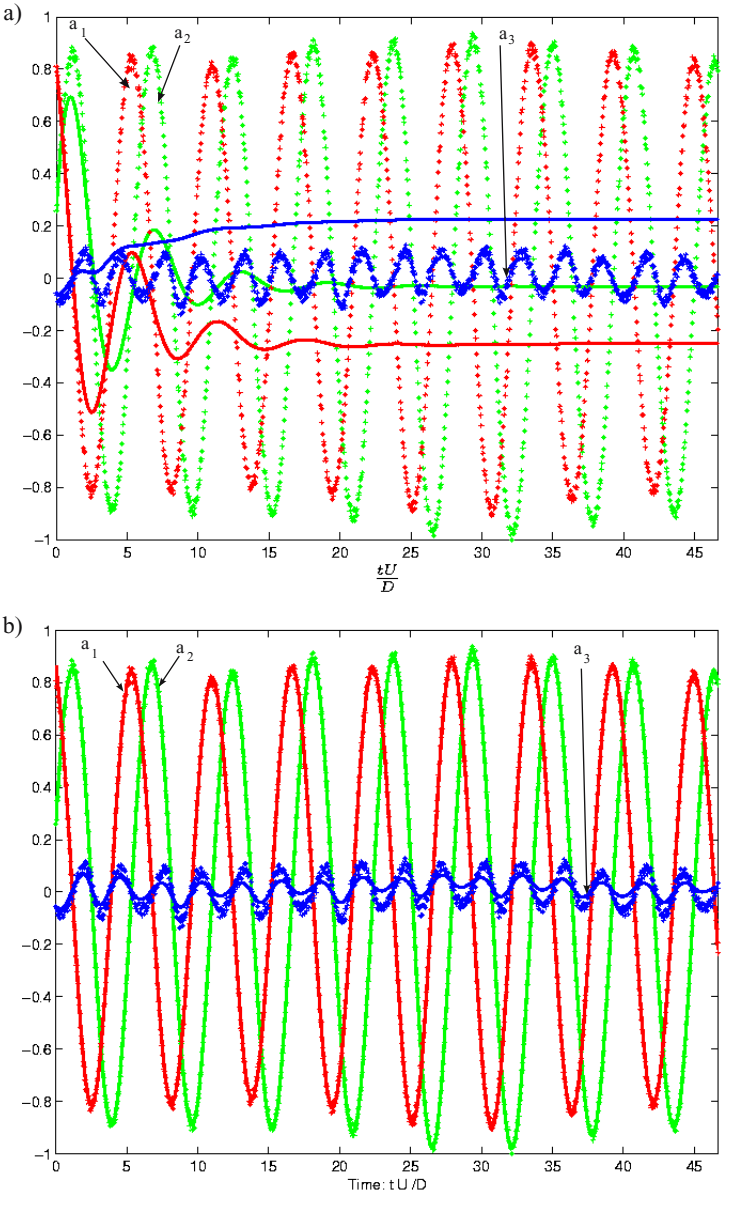

Figure 6. Estimation for a six-mode system. Equation solution in solid line and original data in symbols. (a) POD estimation with strong damping; (b) POD-assimilation result.

case of a six-mode system we estimate an artificial viscosity for the linear term (7) $\nu_A = 2.1\nu$; the corresponding solution is presented in figure 6(a). The inclusion of such artificial vorticity allows the system to remain stable. Even if it has not been possible to obtain a limit cycle for the temporal modes, this solution provides us a reliable first guess for the assimilation technique. Greater values of ν_A produced a too strong damping, and leads to an initial solution

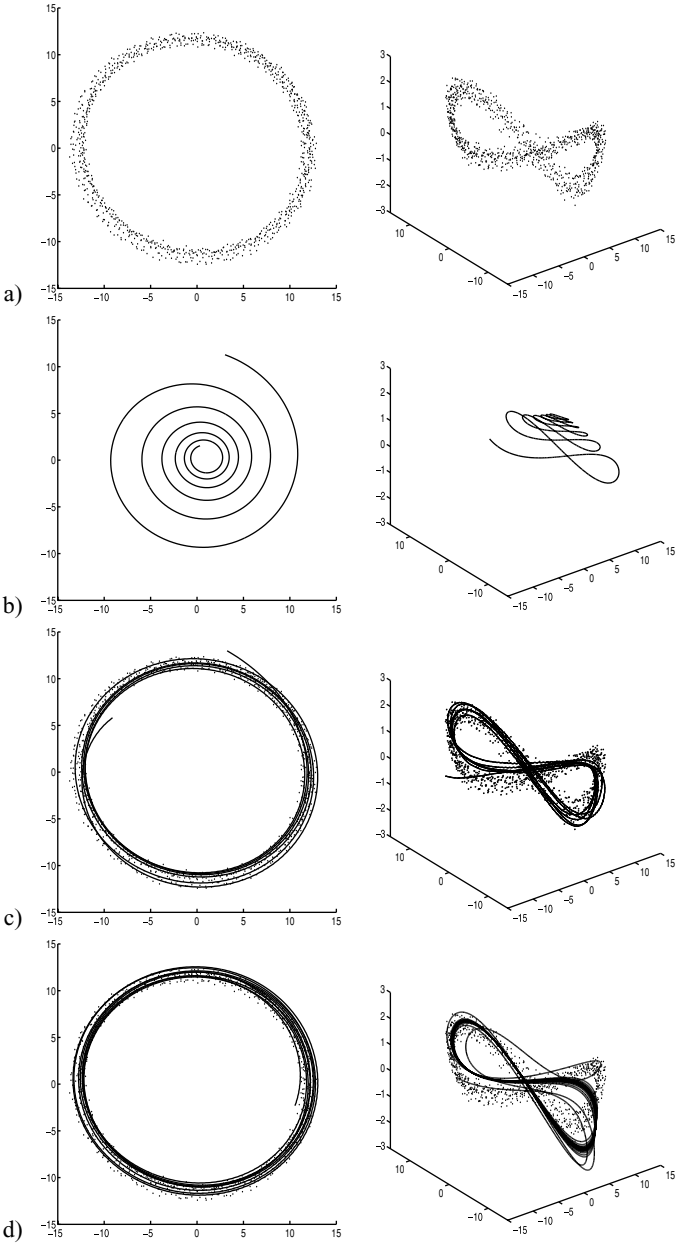

Figure 7. (I) Trajectories of the coefficients of the two principal modes. (II) Trajectories of the coefficients of the three principal modes; (a) 1000 observations; (b) first POD estimation with damping for 1000 images; (c) POD-assimilation result (solid line) compared to observations (symbol); (d) ODE solution from POD-assimilation result (solid line) for 1000 images compared to observations (symbol).

of very bad quality. As can be observed in figure 6(b), even though the considered initial guess was quite far from a good solution, the POD-assimilation method provides a significant improvement.

5.2 *New LODS*

Another important point is that the coefficient matrices I, L and C can be updated from the assimilation results, using the least-squares fit. The initial measurements used to evaluate the matrices are discrete and noisy. As a result of the assimilation process, since the solution provided for $a(t)$ is continuous, the temporal derivatives are much better estimated. Polynomial identification can be performed again to obtain the new coefficient matrices which allow us to recompute new coefficient $a(t)$ through least-squares estimation. We compare in figure 11, for the first two modes, the solution obtained by polynomial identification, the POD-assimilation results and the results of a polynomial identification on the assimilation result.

5.3 *Analysis of phase portraits*

To increase complexity in the flow, a large number of modes were retained in our dynamical system. We have adopted up to those which show an ordered structure in the phase diagram. The resulting dynamical system for three modes presents a trajectory, plotted in figure 7(a), which cannot be confounded with a noise. As the subsequent modes do not exhibit any organized trajectory (figure 8), we excluded them from our analysis. So, an iterative scheme was applied in order to obtain a three-mode LODS.

- Firstly, we used polynomial identification to have a matrix coefficients' estimation (6). To avoid divergence on the ODE solution, damping was introduced in the third linear term of (7) by means of an artificial viscosity. Otherwise, the system solution would diverge after few time steps. Figure 7(IIb) presents this damped result.
- The assimilation algorithm was applied to the bounded solution and by means of polynomial identification in this result, newer matrix coefficients were obtained to refine the model, as previously mentioned in section 5.2. The assimilated curve is presented in figure 7(IIc).
- The first step may restart until a convergence criterion is met.

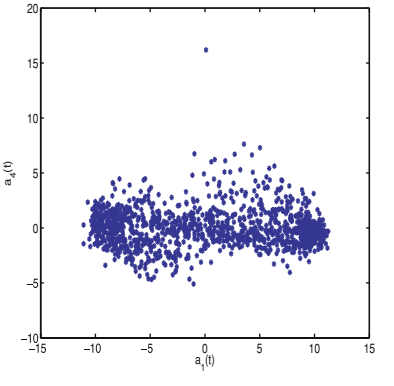

Figure 8. Phase diagram for $a_4(a_1)$. An organized trajectory is not distinguishable.

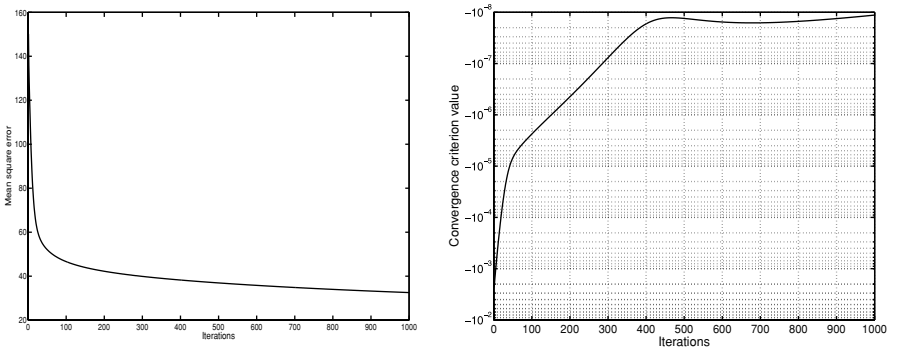

Figure 9. Convergence study: (a) evolution of the mean square discrepancy between estimation and observations; (b) evolution of the convergence criterion.

In order to exhibit these results, the phase portraits of the temporal coefficients are drawn in figure 7. For this case, the best result was achieved with one iteration and a value of artificial viscosity $\nu_A \sim \nu.1$. The two principal modes are recovered during the whole sequence. We can see that the third component of the assimilated curve moves slightly away from the realization trajectory. This is due to the fact that the finer structures of the third mode are computed

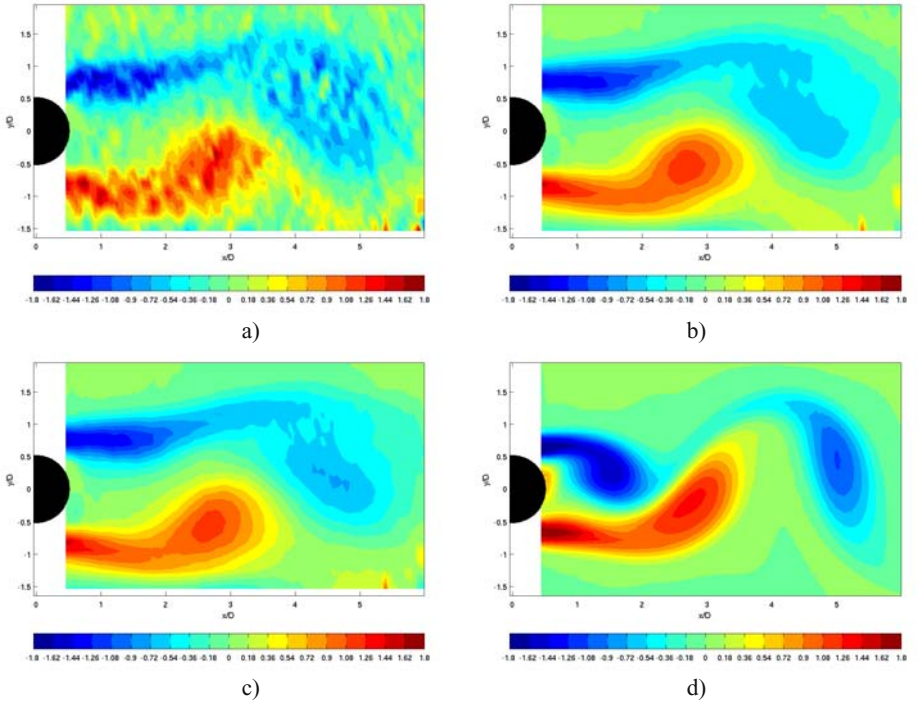

Figure 10. Instantaneous vorticity fields calculated from (a) noisy PIV images; (b) POD reconstruction $s = 6$ modes; (c) POD-assimilation scheme $s = 6$ modes; (d) DNS simulation.

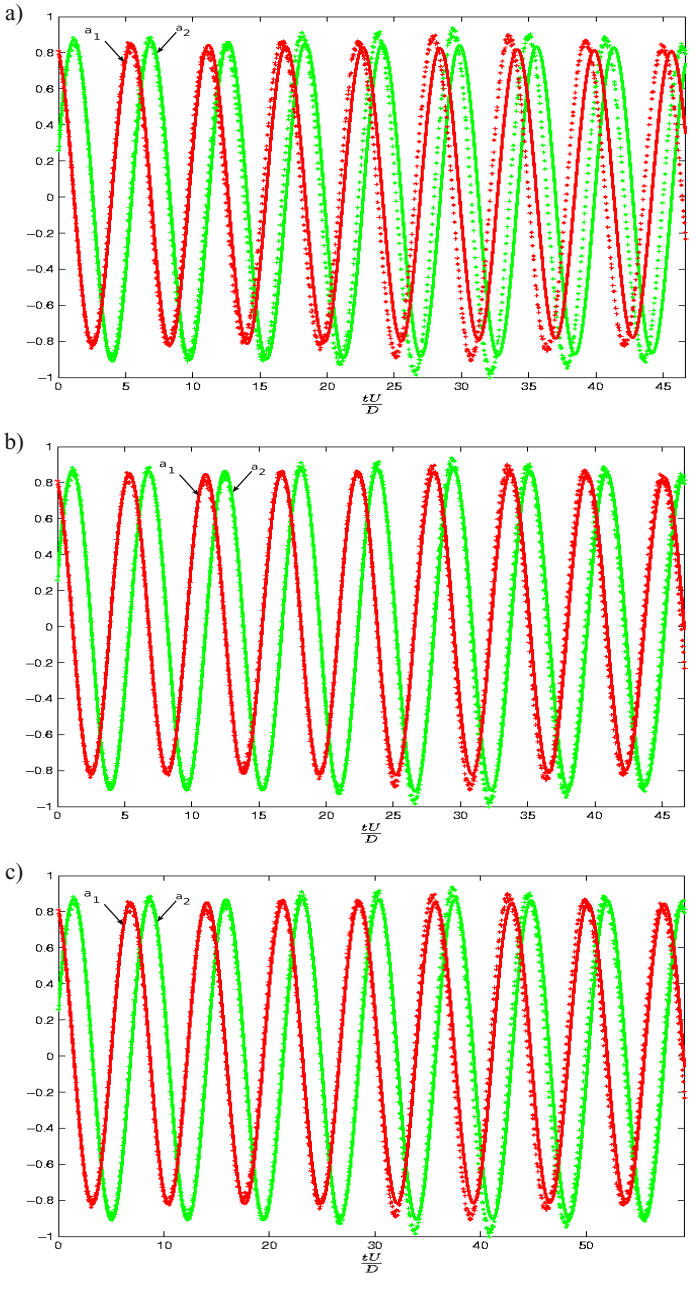

Figure 11. Equation solution in solid line and original data in symbols. (a) POD estimation by polynomial identification; (b) POD-assimilation result; (c) polynomial Identification on the assimilated result.

with less precision than those of the first two modes, as appears in figure 2(b), where more symmetric and organized small structures were expected.

5.4 *Convergence analysis*

The convergence of the assimilation process is experimentally illustrated in figure 9. Both the mean square discrepancy between the estimation and the observation and the

convergence criterion defined in (36) can be computed. In the assimilation method, each iteration enhances the results until the chosen criterion is met. We can see that the $\epsilon = 10^{-7}$ criterion is a good choice, since the iterations could not make the criterion exceed the value 10^{-8}. There is a minimum error due to the observation noise that could not be cancelled out. Indeed, the dynamical equation does not allow discontinuities in the solution, and it can be noticed that the observed modes $s \geq 2$ are more erratic (figure 6(b))

5.5 *Flow reconstruction analysis*

It is remarkable that with $s = 6$ modes, the 94% of the fluctuating kinetic energy is conserved and the LODS produces vorticity snapshots that are in good agreement with the real flow. We compared vorticity fields of original data, POD and POD-assimilation reconstructions in figure 10. It is evident that in this case the POD reduced order model can improve the noisy measures. Even more, the POD-assimilated model exhibits coherent structures closer to a validation case coming from direct numerical simulation (DNS). This DNS of a 2D cylinder flow was conducted for Re $= 125$, in a domain $L_x/D = 19$ by $L_y/D = 12$ with a grid resolution of 685×433. This assures that the grid step $dx \leq \eta$ where η is the Kolmogorov dissipative scale, $\eta \sim \frac{D}{\mathrm{Re}^{3/4}}$. Therefore, every scale of the flow is resolved and the discretization scheme verifies the necessary stability conditions. The code is highly reliable in this regime and its perfomance has been reported previously [12]. The Strouhal numbers $\mathrm{St} = \frac{fD}{U_\infty} \sim 0.2$ issued from simulation (0.1787) and experiments (0.1830) are in good agreement. To evaluate them, we have extracted the dominating frequencies of the lift coefficient from DNS, and the principal frequency of the first modes from POD.

6. Conclusions

Achieving an accurate LODS reconstruction on the basis of experimental data is a much more difficult task than when data considered are issued from numerical simulations. In this work, we have studied the ability of a variational data assimilation method to extract POD-Galerkin LODS from PIV measurements.

The approach followed is partially inspired by a previous scheme [17] that uses the temporal information of the POD decomposition, avoiding the disadvantages of calculus on spatial modes. Tests on PIV noisy experimental data have experimentally demonstrated the efficiency and robustness of the assimilation technique we propose. We chose as a test case a wake flow. The POD-assimilation technique significantly outperforms least-squares fitting methods. Short-term and long-term predictions of good quality have been provided using this method.

Even though the POD-assimilation technique does not provide directly the matrix coefficients that describe the LODS, we have shown in this paper that it does not constitute a limitation of the technique. As a matter of fact, these coefficients can be successfully recovered and enhanced by polynomial identification on the assimilated results.

The reduced order models obtained appear to be a useful tool to correct noisy experimental data. The results of this PIV measurements restoration have been compared to a reliable DNS observations. This research encourages future works on experimental active flow control to be conducted with the help of the POD-assimilation method.

Bibliography

[1] Aubry, N., Holmes, P., Lumley, J.L. and Stone, E., 1988, The dynamics of coherent structures in the wall region of a turbulent boundary layer. *Journal of Fluid Mechanics*, **192**(115), 173, 355.

[2] Bennet, A.F., 1992. Inverse Methods in Physical Oceanography, (Cambridge: Cambridge University Press).

[3] Braud, C., 2003, Etude de la dynamique d'un écoulement à cisaillements croisés: interaction couche de mélange—sillage. Thèse de doctorat (12 décembre 2003), Universite de Poitiers.

[4] Braud, C., Heitz, D., Arroyo, G., Perret, L., Delville, J. and Bonnet, J.P., 2004, Low-dimensional analysis, using POD, for two mixing layer-wake interactions. *International Journal of Heat Fluid Flow*, **25**(3), 351–363.

[5] Cazemier, W., Verstappen, R.W.C.P. and Veldman, A.E.P., 1998, Proper orthogonal decomposition and low-dimensional models for driven cavity flows. *Physics of Fluids*, **10**, 1685.

[6] Couplet, M., Sagaut, P. and Basdevant, C., 2003, Intermodal energy transfers in a proper orthogonal decomposition-Galerkin representation of a turbulent separated flow. *Journal of Fluid Mechanics*, **491**, 275–284.

[7] D'Adamo, J., March 2007, Modelos reducidos para el control de flujos con actuadores EHD, Ph.D. Thesis, Universidad de Buenos Aires.

[8] Deane, A., Kevrekidis, I., Karniadakis, G. and Orszag, S., 1991, Low-dimensional models for complex geometry ows: application to grooved channels and circular cylinders. *Physics of Fluids A*, **3**, 2337–2354.

[9] Everson, R. and Sirovich, L., 1995, The Karhunen-Loeve Procedure for Gappy Data. *Journal of Optical Society of America*, **12**, 1657–1664.

[10] Gerber van der Graaf, GPIV software, http://gpiv.sourceforge.net.

[11] Holmes, P., Lumley, J.L. and Berkooz, G., 1996, Turbulence, Coherent Structures. *Symmetry and dynamical systems* (Cambridge, UK: Cambridge University Press).

[12] Lamballais, E. and Silvestrini, J., 2002, Direct numerical simulation of interactions between a mixing layer and a wake around a cylinder. *Journal of Turbulance*, **3**, 28.

[13] Le Dimet, F. and Talagrand, O., 1986, Variational algorithms for analysis and assimilation of meteorological observations: theoretical aspects. *Tellus*, **38A**, 97–110.

[14] Lumley, J.L., 1967, The structure of inhomogeneous turbulence. In *Atmospheric Turbulence and Radio Wave Propagation*, A.M. Yaglom and V.I. Tatarski, (eds). pp. 166–178 (Nauka: Moscow).

[15] Noack, B.R., Afanasiev, K., MorzyDski, M., Tadmor, G. and Thiele, F., 2003, A hierarchy of low-dimensional models for the transient and post-transient cylinder wake, *Journal of Fluid Mechanics*, **497**, 335.

[16] Perret, L., 2004, Etude du couplage instationnaire calculs expériences en écoulements turbulents. Thesis of the University of Poitiers, France.

[17] Perret, L. Collin, E. and Delville, J., 2006, Polynomial identification of POD based low-order dynamical system. *Journal of Turbulence*, **7**(17), 1–15.

[18] Rajaee, M., Karlson, S. and Sirovich, L., 1994, Low-dimensional description of free shear flow coherent structures and their dynamical behavior. *Journal of Fluid Mechanics*, **258**, 1401–1402.

[19] Rempfer, D., 1996, Investigation of boundary layer transition via Galerkin projection of empirical eigenfunctions. *Journal of Physics Fluids*, **8**(1), 175–188.

[20] Sirovich, L., 1987, Turbulence and the dynamics of coherent structures. Part I-III. Quarterly of *Applied Mathematics*, **XLV**(3), 561–852.

[21] Rabier, F. and Courtier, P., 1992, Four dimensional assimilation in the presence of baroclinic instability. Quarterly *Journal of Royal Metorological Society*, **118**, 649–672.

[22] Rabier, F., Jarvinen, H., Klinker, E., Mahlouf, J.-F. and Simmons, A., 2000, The ECMWF operational implementation of four dimensional variational assimlation. Part I Experimental results with simplified physics. Quarterly *Journal of Royal Metorological Society*, **126**, 1143–117.

[23] Talagrand, O. and Courtier, P., 1987, Variational assimilation of meteorological observations with the adjoint vorticity equation. I. Theory *Journal of Royal Metorological Society*, **113**, 1311–1328.

[24] Willcox, K., 2004, Unsteady flow sensing and estimation via the Gappy proper orthogonal decomposition. In *Proceedings of the 5th SMA Symposium*, January 2004, also AIAA Paper 2004-2415, *Computers and Fluids*, Submitted for publication.